

Supporting Information

Zaid et al. 10.1073/pnas.132292111

SI Materials and Methods

Virus Infections. Epicutaneous infection by scarification was done using 1×10^6 plaque forming units of the HSV-1 KOS strain. Briefly, mice were anesthetized by i.p. injection of a mixture of ketamine (100 mg/kg) and Ilium Xylazil-20 (20 mg/g of body weight) solution in saline. Hair was removed from the left flank of each mouse with clippers and depilation cream (Veet; Reckitt Benckiser) and a small area of skin (2–4 mm²) corresponding with the top of the spleen was lightly scarified using a grindstone tip of a rotary tool (Dremel) for 20 s before inoculation of virus in a 10- μ L volume. The infection site was then covered with a piece of OpSite Flexigrid (Smith & Nephew) and secured with Micropore tape and Transpore tape (3M Health Care) for 48 h following infection. This method of inoculation results in zosteriform spread of virus throughout the dermatome with complete virus clearance by day 8 after infection.

Cell Isolation and Flow Cytometry. Mice were killed by carbon dioxide administration and perfusion was performed with 10 mL Hank's buffered salt solution. Spleens were harvested and disrupted by passage through a wire mesh. Skin tissue (1–2 cm²) was removed after clipping and treatment of flank skin with Veet depilation cream, chopped into small fragments, and incubated for 90 min at 37 °C in 3 mL PBS containing Dispase (2.5 mg/mL; Roche) and DNase (5 μ g/mL; Sigma) followed by incubation for 45 min at 37 °C in MEM medium containing FCS (2%; Gibco BRL), collagenase (3 mg/mL; Worthington), and DNase (5 μ g/mL). Cell suspensions were filtered twice through nylon meshes (70- and 30- μ m pore size) before staining for flow cytometric analysis (30 min at 4 °C). The following antibodies/reagents were purchased from BD Pharmingen: anti-CD103 (M290)-PE and anti-CD45.2 (104)-AlexaFluor 700. Anti- $\gamma\delta$ -TCR (eBioGL3)-APC and anti-EpCAM/CD326 (G8.8)-APC-Cy7 were purchased from Biolegend and anti-CD45.1 (A20)-Pe-Cy7 from eBiosciences. Dead cells were identified using propidium iodide staining. Sphero calibration particles (BD Pharmingen) were added to the samples to allow for calculation of cell numbers. Flow cytometric analysis was performed using a FACSCanto II flow cytometer and FlowJo software (TreeStar).

Immunofluorescence Staining and Confocal Microscopy. Skin from the flank of HSV-infected mice was collected and fixed in phosphate-lysine-paraformaldehyde buffer containing 0.05 M phosphate buffer with 0.1 M L-lysine (pH 7.4; Sigma-Aldrich), 2 mg/mL NaIO₄ (BDH Chemicals), and 4% (vol/vol) paraformaldehyde (Electron Microscopy Sciences, ProSciTech), followed by a rinse in PBS for 10 min and a wash in 10% sucrose (wt/vol in PBS) for 20 min at room temperature (RT). Fixed tissue was embedded in optimal cutting temperature compound (Tissue Tek IA018; Sakura) and frozen in liquid nitrogen. Tissue sections were performed on a cryostat (Leica CM3050S) at 50- μ m thickness and air-dried for 16–18 h before staining. Sections were permeabilized in a 0.5% Triton X-100/ 3% (wt/vol) saponin buffer for 1 h at RT, followed by a PBS wash for 15 min then blocked for 10 min (Protein Block X0909; Dako) at RT. Sections were stained with LM-332 (laminin- γ 2) antibody kindly provided by Monique Aumailley, University of Cologne, Cologne, Germany for 16 h at 4 °C in a semihumid chamber. Sections were rinsed for 10 min in PBS and labeled with donkey anti-rabbit Alexa-Fluor 488 secondary antibody for 40 min at RT. Sections were rinsed for 10 min in PBS, incubated with Hoechst nuclear stain [H33258, 1:3,000 (vol/vol) in PBS] for 3 min, and then mounted

with ProLongGold (P36934; Invitrogen). Images were acquired with a Zeiss LSM700 microscope and processed using Imaris 7 (Bitplane) and ImageJ software.

Intravital Two-Photon Microscopy. Mice were anaesthetized with isoflurane (Cenvet; 2.5% for induction, ~1.5% for maintenance, vaporized in an 80:20 mixture of oxygen and air) using a Tech 3 vaporiser (Surgivet) and the left flank was shaved and depilated using Veet (Reckitt Benckiser). Two parallel incisions were made through the dermis, ~15 mm apart, along the flank. The skin was carefully separated from the peritoneum, and an 18-mm-wide piece of 1-mm stainless steel was inserted under the dermis. This formed a stable raised platform, attached to a custom-made imaging platform. The underside of the dermis was adhered to the steel platform using Vetbond tissue adhesive (3M). Vacuum grease (Dow Corning) was used to attach and seal a glass coverslip onto the epidermis of the skin for imaging. Moist gauze was packed around the incision and covered to prevent dehydration.

Images were acquired with an upright LSM710 NLO multiphoton microscope (Carl Zeiss Microimaging) enclosed in a custom-built environmental chamber (Precision Plastics) that was maintained at 35 °C with heated air. External nondescanned photomultiplier tube detectors in the reflected light path were used to acquire images. Images were acquired with a 20 \times /1.0 N.A. water immersion objective. Fluorescence excitation was provided by a Chameleon Vision II Ti:sapphire laser (Coherent), with dispersion correction. EGFP and DsRed were excited at 900–920 nm. The collagen-rich dermis of the skin was visualized by second harmonic generation, using a bandpass 440- to 480-nm filter. Typical voxel dimensions were 0.55–0.7 \times 0.55–0.7 \times 3 μ m. For four-dimensional datasets, three-dimensional stacks were captured every 1 min for 30–450 min.

Raw imaging data were processed with Imaris 7.5 (Bitplane). Cell migration was analyzed through automatic cell tracking aided by manual corrections. Only tracks that lasted longer than 5 min were analyzed. For assessment of cell morphology (sphericity and area), the 3D surface of the cells was rendered in Imaris. Overlay of image sequences and assessment of 2D cell area was calculated using ImageJ. Colocalization was performed using Imaris. Data were used to plot graphs in Prism 5 (Graphpad). For the generation of movies, image sequences exported from Imaris were composed in Adobe After Effects CS5.

Simulating Cell Migration and Diffusion in the Skin. To determine the rate of change of the concentration of cells within a rectangular strip of skin, the movement of cells was modeled conceptually by sampling with replacement from a dataset of observed displacements per minute of individually tracked *in vivo* cells. By the central limit theorem, and confirmed by numerical experiments, the distribution of the displacement of a cell over a period of t minutes converges quickly to a Gaussian distribution for t much larger than 1. Because the time period of interest is large (over 100 d, or 144,000 min), essentially identical answers are obtained by modeling the movement of cells by a Wiener process appropriately fitted to the displacement data.

Let $p(x, y; t)$ denote the proportion of cells at the point $(x, y) \in \mathbb{R}^2$ at time $t \in \mathbb{R}$. By definition of proportion, $\iint p(x, y; t) dx dy = 1$ for all t . The displacement of a single cell in the xy plane after t minutes has the 2D Gaussian distribution $N_2(0, \sigma^2 t I)$ where I is the identity matrix and σ is related to the average displacement per minute v by $v = \sqrt{\pi/2} \sigma$. Therefore,

$$p(x, y; t) = \int_{-\infty}^{\infty} \int_{-\infty}^{\infty} p(x-x', y-y'; 0) \frac{1}{2\pi\sigma^2 t} \exp\left(-\frac{x'^2 + y'^2}{2\sigma^2 t}\right) dy' dx'.$$

$$\int_{-L}^L p(x; t) dx = \operatorname{erf}\left(\frac{L}{\sqrt{2\sigma^2 t}}\right).$$

Of primary interest is the marginal distribution $p(x; t) = \int_{-\infty}^{\infty} p(x, y; t) dy$ obtained by averaging over the y coordinate. A standard calculation shows that

$$p(x; t) = \int_{-\infty}^{\infty} p(x-x'; 0) \frac{1}{\sqrt{2\pi\sigma^2 t}} \exp\left(-\frac{x'^2}{2\sigma^2 t}\right) dx'.$$

In particular, this shows that the problem reduces to studying a one-dimensional Wiener process.

If all of the cells start at the origin [meaning $p(x; 0)$ is the Dirac delta function] then the density evolves according to

$$p(x; t) = \frac{1}{\sqrt{2\pi\sigma^2 t}} \exp\left(-\frac{x^2}{2\sigma^2 t}\right).$$

Because the distribution is Gaussian for $t > 0$, this equation can also be used for determining how the distribution evolves assuming the initial distribution is zero-mean Gaussian. (If the initial distribution is zero-mean Gaussian with variance ϕ^2 then define $t_0 = \phi^2/\sigma^2$; note that the variance of $p(x; t_0)$ is ϕ^2 . After another t minutes, the distribution has evolved from $p(x; t_0)$ to $p(x; t_0 + t)$.) Furthermore, the proportion of cells within a strip from $-L$ to L is

To determine a suitable value of σ , a dataset was used of 30 tracked cells over a period of 2 h. The dataset recorded the 2D location of each cell at intervals of 1 min. (Actually, the 3D location was recorded, but it suffices to ignore the depth axis.) After discarding the few occasions when the position of a cell could not be determined accurately, there remained 3,512 measured displacements. The empirical variance of these 2D displacements is

$$\begin{pmatrix} 0.70 & 0.01 \\ 0.01 & 0.80 \end{pmatrix}.$$

Had the displacements been perfectly radially symmetric, the covariance matrix would have been of the form

$$\begin{pmatrix} \sigma^2 & 0 \\ 0 & \sigma^2 \end{pmatrix}.$$

If it is assumed that the true distribution really is radially symmetric—a cell is equally likely to move in any direction in the xy plane—then an estimate of σ^2 is 0.75. [If $Z \sim N_2(0, \sigma^2 I)$ then $\mathbb{E}(\|Z\|^2) = 2\sigma^2$. The sample average of $\|Z\|^2$ is 1.5, therefore a reasonable estimate of σ^2 is 0.75.] Regardless, the variance σ^2 of the displacement along a single axis in the xy plane is somewhere in the vicinity of 0.7–0.8, corresponding to an average displacement per minute of 1.05 $\mu\text{m}/\text{min}$ to 1.12 $\mu\text{m}/\text{min}$.

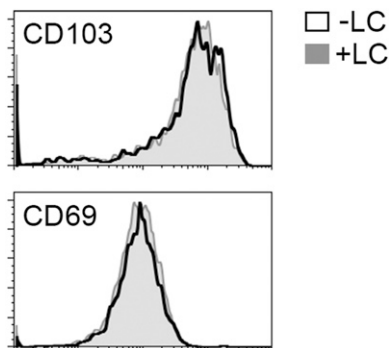


Fig. S1. Expression of CD103 and CD69 on gBT-1 T_{RM} after Langerhans cell (LC) ablation from Lg-DTR mice. Thirty days after HSV infection, Lg-DTR mice were treated with diphtheria toxin or PBS for 2 wk, as described in *Materials and Methods*. $n = 5$ –11 mice per group.

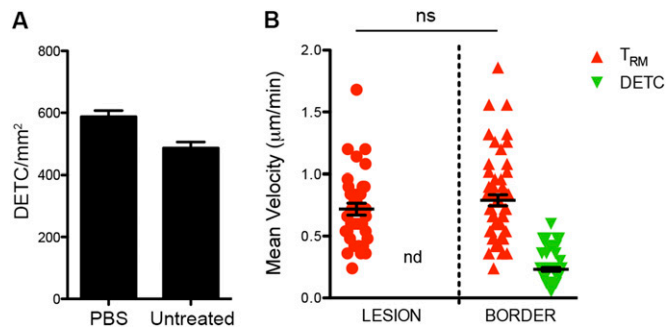


Fig. 52. (A) Dendritic epidermal $\gamma\delta$ T cell (DETC) numbers in the skin of CXCR6^{GFP/+} mice 28 d after intradermal injection of PBS, as described in *Materials and Methods*. Higher numbers of DETCs were observed in the skin after PBS injection, compared with untreated skin. $n = 4-6$. (B) Mean velocity of gBT-I.DsRed tissue-resident memory T cells (T_{RM}) and CXCR6^{GFP/+} DETC within the indicated regions relative to the site of infection (lesion) in the skin 30 d after HSV infection. ns, not significant. Error bars represent SEM.

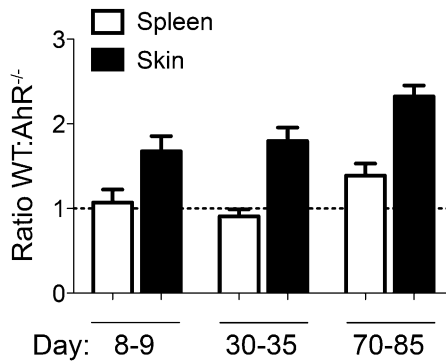
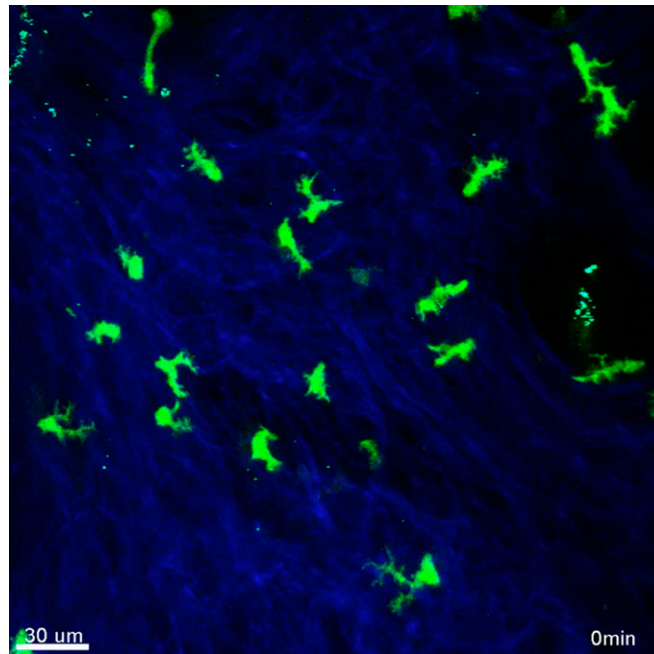
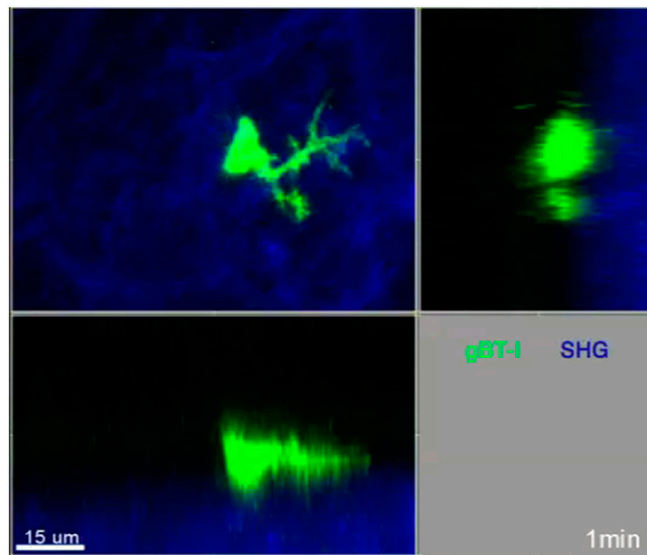


Fig. 53. Ratio of WT to Ahr^{-/-} CD8⁺ T cells in the skin or spleen at the indicated times after intradermal transfer of equal numbers of effector T cells. Error bars represent SEM. Data pooled from two to three experiments with three to five mice per group.



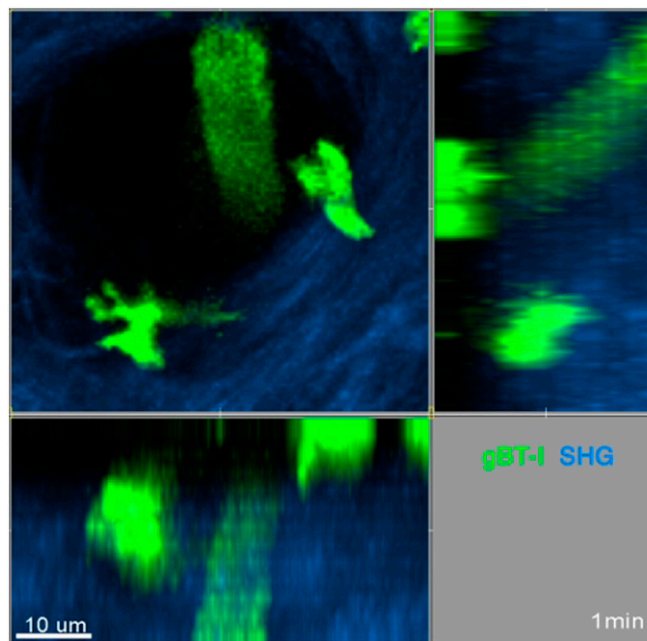
Movie S1. Epidermal CD8⁺ T_{RM} migrating in the skin 32 d after HSV infection. A maximum intensity projection time series of gBT-I.GFP T cells (green) imaged by two-photon microscopy. The collagen-rich dermis was visualized by second harmonic generation (SHG; blue). Frames were acquired at 1-min intervals. Display rate: 10 frames per second (fps).

[Movie S1](#)



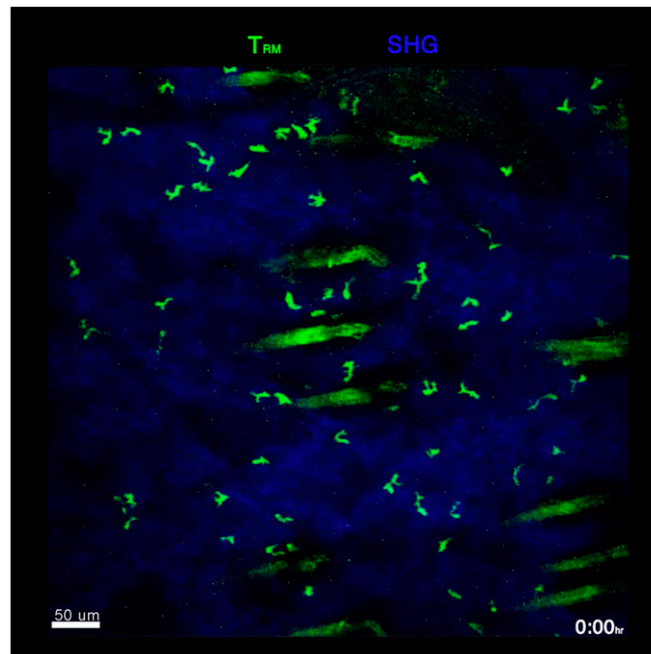
Movie S2. Skin T_{RM} project dendrites laterally as they migrate, and not upward toward the apical epidermis or downward toward the dermis. A maximum intensity projection (in x - y , x - z , and y - z dimensions) of an epidermal $CD8^+$ T-cell migrating in the skin 32 d after HSV infection. gBT-I.GFP T cells (green) were imaged by two-photon microscopy. The collagen-rich dermis was visualized by SHG (blue). Frames were acquired at 1-min intervals. Display rate: 10 fps.

[Movie S2](#)



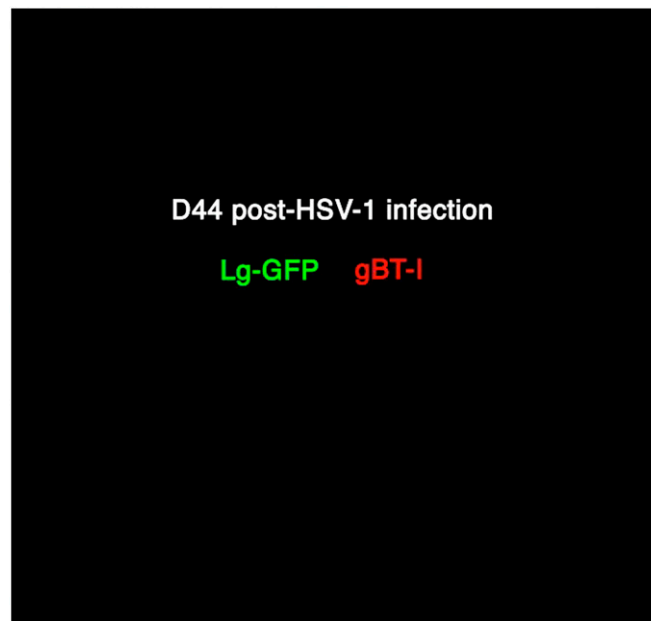
Movie S3. Skin T_{RM} enter hair follicles while migrating in the epidermis. A maximum intensity projection (in x - y , x - z , and y - z dimensions) of an epidermal $CD8^+$ T-cell (red asterisk) migrating from the epidermis into a hair follicle. gBT-I.GFP T cells (green) were imaged by two-photon microscopy 32 d after HSV infection. The collagen-rich dermis was visualized by SHG (blue). Frames were acquired at 1-min intervals. Display rate: 10 fps.

[Movie S3](#)



Movie S4. Time-lapse imaging of epidermal CD8⁺ T_{RM} migrating in the skin reveals low-speed immunosurveillance. A maximum intensity projection time series of gBT-I.GFP T cells (green) imaged by two-photon microscopy for 7.5 h. The collagen-rich dermis was visualized by SHG (blue). Frames were acquired at 3-min intervals and all frames overlaid to produce the composite image shown at the end of the video. Display rate: 10 fps.

[Movie S4](#)



Movie S5. Skin T_{RM} interact regularly with LCs as part of their migration program. In the first part of the video, gBT-I.DsRed T cells (red) were imaged alongside LCs in Langerin-GFP mice 44 d after HSV infection. Three examples of contacts between T_{RM} and LCs demonstrated by a colocalization channel (white) are shown in the next part of the video. The final part of this video shows skin T_{RM} in Langerin-DTR mice 2 wk after depletion of LCs by diphtheria toxin treatment. Frames were acquired at 1-min intervals. Display rate: 10 fps.

[Movie S5](#)

